

# Hepatoprotective Effect of Yiqijianpi Formula (YQJPF) on Liver Failure Through Modulation of Hypoxic and Apoptosis Pathways

**Li Tang**

Nanjing University of Chinese Medicine

**Feixia Wang**

NANJING UNIVERSITY OF CHINESE MEDICINE

**Lingyan Xiao**

The Second Affiliated Hospital of Nanjing University of Chinese Medicine

**Min Shen**

Nanjing University of Chinese Medicine

**Siwei Xia**

Nanjing University of Chinese Medicine

**Zili Zhang**

Nanjing University of Chinese Medicine - Hanzhongmen Campus

**Feng Zhang**

Nanjing University of Chinese Medicine

**Shizhong Zheng**

Nanjing University of Chinese Medicine

**Shanzhong Tan** (✉ [20195183@njucm.edu.cn](mailto:20195183@njucm.edu.cn))

Nanjing hospital affiliated to Nanjing university of Chinese Medicine

---

## Research

**Keywords:** Yiqijianpi decoction, Acute on chronic liver failure, Network pharmacology, Apoptosis, Hypoxic liver injury

**Posted Date:** December 10th, 2020

**DOI:** <https://doi.org/10.21203/rs.3.rs-122878/v1>

**License:** © ⓘ This work is licensed under a Creative Commons Attribution 4.0 International License. [Read Full License](#)

---

# Abstract

## Background

Acute-on-chronic liver failure (ACLF) is a severe complication of cirrhosis, which seriously endanger human life and health. Yiqijianpi decoction (YQJPF) is a Traditional Chinese Medicine (TCM) formula that has been widely used in the treatment of liver failure with significant effect. The purpose of this study was to investigate the active components and mechanism to ameliorate acute on chronic liver failure(ACLF).

## Methods

LPS combined with D-Gal was used to establish the rat model of ACLF, pathological examination was detected by H&E staining, liver function test was assayed by ELISA. LPS was used to induce hepatocytes injury in vitro. Cell proliferation assay, TUNEL assay were used in human hepatic L02 cells. The active components and putative targets of YQJPF were predicted by network pharmacology approach and GEO analysis. Functional and pathway enrichment analysis were presented by using String, Cytoscape and Metascape. Further, experimental validation was done to verify the effect of YQJPF on PI3K/AKT-HIF-1 $\alpha$  and apoptosis-related signaling pathways by using Immunohistochemistry and Western blotting.

## Results

After being treated with YQJPF, the rat liver injury and fibrosis were alleviated, and Cell Counting Kit-8 assay, TUNEL assay indicated YQJPF also inhibited the apoptosis in hepatic L02 cells. Through network pharmacologic analysis, 135 active components in YQJPF decoction, 573 known therapeutic targets and 2940 liver failure-related human genes were identified. 163 gene symbols maybe the key for liver failure treatment by YQJPF decoction. VEGF-A was hub gene in PPI network. The KEGG pathway and GO enrichment analyses indicated that the PI3K/AKT, HIF-1 signaling pathways were the prominently enriched signaling pathways. In vivo, YQJPF upregulated the expression of PI3K/AKT-HIF1- $\alpha$  and VEGF-A. Moreover apoptosis pathway were verified by up-regulating Bcl2 expression and down-regulating Bax expression in vivo and in vitro.

## Conclusion

YQJPF is beneficial for alleviating liver failure, may regulate hypoxic liver injury through PI3K/AKT-HIF1 $\alpha$  dependent apoptosis pathway.

# 1. Introduction

Liver failure is the critical condition, the incidence of the disease has an increasing tendency with alcohol abuse or alcoholism, and growing epidemic of obesity, diabetes, which have long plagued the medical profession<sup>[[i]]</sup><sup>[[ii]]</sup>. Liver failure mainly concludes acute liver failure (ALF), acute-on chronic liver failure (ACLF), or an acute decompensation of an end-stage liver disease, in some cases they have some common pathological process, liver cell damage runs through the entire course of disease development<sup>[[iii]]</sup>. Among them ACLF is a syndrome of hepatic decompensation <sup>[[iv]]</sup><sup>[[v]]</sup>, although there are existed some disputes on its clinical definition, in general, it is a distinct entity where acute damage to liver function on the basis of chronic liver disease or cirrhosis patient, which could cause acute hepatic decompensation with a high short-term mortality. It seriously threatens the lives of patients with chronic liver disease<sup>[[vi]]</sup><sup>[[vii]]</sup>. However, no effective therapy for liver failure beyond supportive treatment is currently available, as such, the search for a new treatment or medicine against liver failure is still needed.

Traditional Chinese Medicine (TCM) has been widely used for the treatment of liver failure with a long history. Yiqijianpi formula(YQJPF) is used to treat ACLF patients based on the TCM theory of 'Strengthening body resistance', it composes 9 herbs: Astragalus membranaceus (Huang Qi), and Radix pseudostellariae (Tai Zishen) are Monarch drugs. Angelica sinensis (Dang Gui), Fructus Ligustri Lucidi (Nv Zhenzi), Poria Wolfiporia extensa (Fu Lin), Atractylodes macrocephala (Bai Zhu) are Ministerial drugs, Pericarpium citri reticulatae (Chen Pi), Scutellaria baicalensis (Huang Qin), Glycyrrhiza uralensis (Gan Cao) are adjuvants, they work together to play the role of nourishing Qi and Yin, regulating Qi and clearing away heat. Of these herbs, Astragalus membranaceus<sup>[[viii]]</sup><sup>[[ix]]</sup>, Radix pseudostellariae<sup>[[x]]</sup><sup>[[xi]]</sup>, Atractylodes macrocephala<sup>[[xii]]</sup> provide significant protection against organ injury in various disease models. The active compounds in Angelica sinensis<sup>[[xiii]]</sup>, Scutellaria baicalensis<sup>[[xiv]]</sup> and Fructus Ligustri Lucidi<sup>[[xv]]</sup> have been proved to remit hepatic injury. YQJPF has proved to be a safe and effective formulation according to preliminary clinical study, which can further improve clinical efficacy in the treatment of ACLF<sup>[[xvi]]</sup>, it could significantly ameliorate the biochemical indicators and MELD scores, and lower the mortality. The ingredients in YQJPF are complex, and the pharmacological mechanism needs to be further explored. Further research on the mechanism of YQJPF can provide scientific basis for the treatment of patients with liver failure.

This study we investigated the effect of YQJPF on hepatocyte in vitro and in vivo, and a network pharmacology analysis<sup>[[xvii]]</sup> was performed to explore the potential molecular mechanisms. (**Figure abstract**).

# 2. Materials And Methods

## 2.1 YQJPF decoction Preparation

The YQJPF decoction contained 30 g of Astragalus membranaceus, 30 g of Radix pseudostellariae, 30 g of Angelica sinensis, 10g of Fructus Ligustri Lucidi, 15 g of Poria Wolfiporia extensa, 15 g of Atractylodes macrocephala, 3 g of Pericarpium citri reticulatae, 10g of Scutellaria baicalensis, 10 g of Glycyrrhiza uralensis. All the herbs were obtained from Nanjing Hospital Affiliated to Nanjing University of Chinese Medicine ( Nanjing, China ). HPLC analysis was

performed against a known herbal standard further verifying herb identity and its active components. Each formula was resuspended in deionized water and incubated at 80 °C for 30 min. The supernatant was separated from any insoluble material by centrifugation (3000 g, 20 min) followed by passage through a 0.22 µm filter. The concentration of herbal supernatant was based on the dry weight of herb per unit volume. For the in vitro cell culture studies, 28.8 mg/mL YQJPF extract was prepared, while 2.86 g/mL YQJPF was used for the in vivo animal experiments.

## 2.2 Establish ACLF rat model

Sprague-Dawley rats (males, 180-220g) were purchased from Beijing Vital River Laboratory Animal Technology Co., Ltd. (Beijing, China). The rats were housed at 24±1°C under a 12-h light/dark cycle with free access to food and water. The rats were randomly assigned to two groups, the control group (Control, n=6) and the model group (Model, n=24). The rats in the Model group were intraperitoneally injected with 50% CCl<sub>4</sub> in an olive oil solution at 1mL/100g body weight twice a week for 12th weeks. At the end of the eighth week, the rats in the CCl<sub>4</sub>-treated group were randomly divided into four groups: the ACLF model group (ACLF Model, n=6), the low-dose YQJPF group (YQJPF 14.3g/kg, n=6), the high-dose YQJPF group (YQJPF 28.6g/kg, n=6) and methylprednisolone treatment group (MP 15mg/kg, n=6). The methylprednisolone group was given methylprednisolone 15mg/kg by intravenous injection. The rats in Control group were administered with the corresponding amount of saline. At the end of the 12th week, LPS (100 ug/kg) and D-Gal (400 mg/kg) were used to induce acute liver injury except the Control group. All rats were sacrificed when 24 hours after acute injury, and the liver samples were collected for subsequent research and analysis.

## 2.3 Liver histopathological analysis

Rat liver tissues were collected after sacrifice, then weighed before sectioned into small pieces, fixed them in 4% paraformaldehyde and subjected to paraffin embedding for haematoxylin and eosin (H&E) staining.

## 2.4 Biochemistry analysis for liver injury

The contents of AST and ALT in liver tissues were measured according to the instructions of the corresponding Alanine aminotransferase Assay Kit and Aspartate aminotransferase Assay Kit (Nanjing Jiancheng Bioengineering Institute, Nanjing, China).

## 2.5 Cell Culture

Human L0<sub>2</sub> cell line was brought from Cell Bank of Chinese Academy of Sciences (Shanghai, China). Cells were cultured in DMEM with 10% FBS, 1% antibiotics, and incubated in a 5% CO<sub>2</sub> and 95% air humidified atmosphere at 37 °C.

## 2.6 Cell viability assay

Cellular viability was detected by the Cell Counting Kit-8 (APEX BIO, USA). Cells were cultured in 96-well plate at 100 µl volume per well. After drugs administration, 10 µl CCK8 solution was added in the cell culture medium and incubated for 1.5h at cell incubator. The absorbance of each well was determined at 450 nm by a Microplate Reader (Bio-Rad, Hercules, CA, USA).

## 2.7 Cell apoptosis detection

Cell apoptosis was detected by the Apoptotic/Necrotic Cell Detection Kit (BestBio, Shanghai, China). The blue fluorescence density was measured by fluorescence microscope (Nikon, Tokyo, Japan).

## 2.8 Network Pharmacology

### 2.8.1 Analysis of YQJPF active compounds and disease targets

The active compounds in YQJPF were obtained from two distinctive TCM databases, namely Traditional Chinese Medicine Systems Pharmacology Database and Analysis Platform (TCMSP; <http://lsp.nwu.edu.cn/tcmsp.php>, ver. 2.3) and Traditional Chinese Medicine Integrated Database (TCMID, <http://www.megabionet.org/tcmid/>). The pharmacokinetic and pharmacodynamic parameters should meet the following criteria: oral bioavailability (OB) ≥30% and drug-likeness (DL) ≥ 0.18 in TCMSP. Because Glycyrrhiza uralensis was used as an adjuvant in the YQJPF, the candidate compounds in it should meet the criteria of OB ≥50% and DL ≥0.18. In addition, combined with HPLC, Chinese National Knowledge Infrastructure (CNKI), Pubmed database, some chemical components that failed to meet the criteria, but reported to have biological and pharmacological effects were also included as candidate active components for further analysis.

The corresponding targets of these compounds were searched in the TCMSP and Swiss Target Prediction (<http://www.swisstargetprediction.ch/>) databases. The gene symbols were obtained from the UniProtKB database (<http://www.uniprot.org>) with the selected species as Homo sapiens. After deletion of redundant items, the final herb-active compounds-targets network graphs were constructed and visualized using Cytoscape v3.7.1.

Liver failure targets were predicted and screened using the GEO database, two gene expression profiles, GSE14668 and GSE38941, which contained microarrays of liver tissue samples from liver failure patients and normal liver donor tissue samples, were chosen for further analysis. The data in these two profiles were obtained from the GPL570 [HG-U133\_Plus\_2] (Affymetrix Human Genome U133A array) platform and were initially analyzed with GEO2R. A fold-change was regarded as significant with P<0.05 and with threshold values>1.0 or <-1.0. The co-expression of differentially expressed genes (DEGs) were identified to establish the liver failure-related targets data.

### 2.8.2 Compound-Target-Disease Network Construction and Enrichment of KEGG/GO Pathways

Venny 2.1.04 (Venny, 2018) was used to screen for common targets between YQJPF and disease-related targets. Then we inputted the intersected gene symbols into String (Search Tool for the Retrieval of Interacting Genes/Proteins, Version: 10.5, <http://string-db.org/>), which was used to search for and predict protein interactions. The analysis results were imported into Cytoscape 3.7.1 to analyze and draw the Protein–Protein Interaction (PPI) Network. Hub targets were ranked by degree values to construct a hub gene targets network and a compound-target network for YQJPF on liver failure.

In order to further explain the potential mechanism of YQJPF Decoction in treating liver failure. Gene ontology (GO) analysis and Kyoto Encyclopedia of Genes and Genomes (KEGG) Pathway were performed using Metascape.

## 2.9 Western blot assay

Liver tissue homogenates were ultrasonic splitted and centrifuged at 12000 revolutions per minute for 15 min at 4°C to separate the membrane-containing fraction (pellet) from the cytosolic fraction. Western blot analysis was conduct according to the manufacturer's instructions (Bio/Rad, Hercules, CA, USA), then immunoblot with rabbit anti-Actin (1:1000 dilution, #ab8226, Abcam), rabbit anti-Phospho-PI3K (Tyr607, 1:1000, AF3241, Affinity Biosciences Inc, China), rabbit anti-Phospho-AKT (Thr308, 1:1000, #13038, Cell Signaling Technology), rabbit anti-HIF-1 $\alpha$  (1:1000, #3716, Cell Signaling Technology), rabbit anti-VEGF-A (1:1000, ab46154, Abcam), rabbit anti Bcl-2 (1:1000, ab32124, Abcam) and rabbit anti Bax (1:1000, ab182733, Abcam).

## 2.10 Immunohistochemistry

Liver tissues were fixed with 10% paraformaldehyde for 12h and then embedded in paraffin. Embedded paraffin sections were de-waxed in xylene and rehydrated in ethanol. Antigen retrieval was performed in 0.01M citrate buffer (pH 6.0) using a pressure cooker followed by incubation for 3 min. Samples were then washed thrice with PBS and fixed in 95% ethanol for 30 min. Immunohistochemical staining was performed using antibodies against HIF-1 $\alpha$ , VEGF-A as previously described.

## 2.11 Statistical Analysis

Data were presented as the mean  $\pm$  SD. The significance of results was determined based on one-way ANOVA analysis using Prism 8.0.1 (Graphpad, San Diego, CA, USA).  $P < 0.05$  was considered significant. All experiments were repeated at least three times.

# 3. Results

## 3.1 YQJPF preserved liver failure in vivo

Establish ACLF model on SD rat as previously described[[i]]. The pathological changes in liver tissues were evaluated with H&E staining. The livers were rosy and smooth with intact lobule structure in the Control group. However, the livers in the ACLF Model group became small and hard accompanied by necrosis, with small nodules on their surface (**Fig. 1A**). As shown in **Fig. 1B**, the liver tissue of rats in the Control group was well-organized and the liver cells were intact. In the ACLF Model group, the liver tissue structure was disordered, and the fibrous tissue was obviously proliferated, accompanied by a large number of inflammatory cell infiltration, pseudolobule formation, large and sub-large hepatocyte necrosis, vacuolation, dilation and congestion of hepatic sinusoids. The liver tissue fibrosis in the YQJPF group and Methylprednisolone group was improved, the number of inflammatory cell infiltration and pseudolobule formation were reduced compared with the Model group, so was the hepatocyte necrosis and vacuolation.

As shown in Masson staining (**Fig. 1C**), in the Control group, only a small amount of collagen staining was seen on the blood vessel wall. The collagen deposition in the ACLF Model group was significantly increased. Collagen fibers were found to form filaments or even thick cords around the sinuses. The structure of liver lobules was disordered and fibrous tissue proliferation was also seen. After YQJPF and methylprednisolone treatment, collagen deposition and collagen volume fraction were significantly improved compared with the ACLF Model group .

Sirius staining results showed that the liver tissues in the Model group were severely fibrotic (**Fig. 1D**), and there was a large amount of red collagen-like fibrous material deposited around the liver tissue portal area. Compared with the Model group, the red fiber-like material around the liver tissue portal area, and the bold duct of the treatment group were significantly reduced after YQJPF and methylprednisolone treatment.

Levels of AST and ALT were detected to assess the damage of hepatocytes. Liver tissue levels of ALT and AST were increased significantly in the Model group. The levels of these enzymes were decreased in YQJPF treatment group and methylprednisolone group. Thus, YQJPF exerted a protective effect on liver damage in ACLF.

## 3.2 YQJPF impress Hepatocyte proliferation and apoptosis in Liver Injury

In order to further explain the mechanism of YQJPF, we selected L0<sub>2</sub> human hepatocyte cell line for further analysis, LPS (4  $\mu$ g/ml) induced to establish a liver injury model, and then YQJPF (10 $\mu$ g/ml, 20 $\mu$ g/ml, 40 $\mu$ g/ml) intervent for 24 hours to verify the effect. Cell Counting Kit-8 analysis showed that YQJPF could dose-dependently attenuates cell viability (**Fig. 2A**). Apoptosis morphology was detected with fluorescence microscopy, it implied that LPS induce apoptosis in hepatocytes and YQJPF could inhibit apoptosis (**Fig. 2B**). In the LPS-induced Model group, the expression of Bax was increased, while the production of Bcl-2 was dramatically reduced compared to that in the Control group. YQJPF activates Bcl2, reduces BAX, and shifts the BAX/Bcl2 ratio in a anti-apoptotic direction (**Fig. 2D**). CCK-8 analysis indicated that YQJPF 20 $\mu$ g/ml have the analogous effect as apoptosis inhibitor Z-VAD-FMK to restore cell viability (**Fig. 2C**). Overall YQJPF could promote hepatocyte proliferation, and influence the apoptosis.

## 3.3 Network Pharmacology

### 3.3.1 Screening of Active Components in YQJPF

The fingerprint of the water extract of YQJPF was performed by high performance liquid chromatography (HPLC) (**Fig. 1A**). The four main peak compounds in the HPLC were identified as Calycosin-7-O- $\beta$ -D-glucoside, Ferulic acid, Hesperidin, Glycyrrhizic acid.

By a comprehensive search of the TCMS, a list of components in YQJPF was obtained, after ADME screening (OB  $\geq$  30%, OB(Glycyrrhiza uralensis)  $\geq$  50%; DL  $\geq$  0.18), 117 active components in YQJPF matched the combined filtering criteria which integrated by OB and DL. 15 components, like Resveratrol, Astragalus polysaccharide, Licopyranocoumarin, etc, confirmed as the bioactive components of the herb medicines according to previous researches, simultaneous determination of four bioactive compounds in YQJPF extracts by high performance liquid chromatography. Other components were obtained from TCMID database (**Supplementary Table S1**).

For further analysis, there were totally 135 active components in 9 herbs, among them 24 active components in Astragalus membranaceus (Huang Qi), 18 active components in Radix pseudostellariae (Tai Zishen), 15 active components in Angelica sinensis (Dang Gui), 12 active components in Fructus Ligustri Lucidi (Nv Zhenzi), 11 active components in Poria Wolfiporia extensa (Fu Lin) and 9 in Atractylodes macrocephala (Bai Zhu), 6 in Pericarpium citri reticulatae (Chen Pi), 31 in Scutellaria baicalensis (Huang Qin), 25 active components in Glycyrrhiza uralensis (Gan Cao). In addition, 14 active components were common ingredients in more than two herbs (**Table S2**).

### 3.3.2 The Potential Targets of Active Compounds in YQJPF

The active compound targets were searched via the TCMS and Swiss Target Prediction databases for each chemical component. The targets were transformed using the UniProt knowledge database, data were merged to obtain gene symbols. After eliminating the redundant targets, a total of 573 known therapeutic targets were collected from 135 compounds (**Tables S3-S11**). For further analysis, a Compound-Target network was visualized using Cytoscape. The network contains 715 nodes and 2979 edges. Among them 135 nodes represented the active components, and 573 nodes represent the corresponding targets of the ingredients (**Fig. 3B**). The Compound-Target network showed that a herb could interact with multiple components, and a compound could also interact with several targets, which coincided with the synergistic effect theory of multi-components and multi-targets of traditional Chinese medicine formula. The degree (connection strength) was reflected by the node's sizes, according to the degree value, **Fig. 3C and Table S12-13** showed the top 10 active components and targets.

### 3.3.3 Acquisition of Therapeutic Gene Targets for Liver Failure

To investigate the therapeutic gene targets in liver failure, we analyzed the expression profiles data from GEO database. We applied the GEO2R online analysis tool with default parameters to screen the differentially expressed genes (DEGs) in two GEO series (GSE14668, GSE38941), using adjusted P value  $< 0.05$  and  $\log_{2}FC \leq -1$  or  $\log_{2}FC \geq 1$  as the cut-off criteria. Two GEO series contains 18 normal and 25 liver failure samples. **Fig. 4A-4B** showed the up-regulated genes and down-regulated genes. Venn diagram identified 2961 common DEGs in two GEO series. 21 DEGs with inconsistent trends had been excluded. Overall, 2940 DEGs were obtained, including 1760 up-regulated and 1180 down-regulated genes (**Fig. 4C, Table S14-16**).

### 3.3.4 Potential Targets of YQJPF Decoction on Liver Failure

Venn diagram showed that 2940 gene symbols for disease and 573 gene symbols for drugs had 163 overlap. That was, 163 gene symbols would mostly likely to be the therapeutic targets for liver failure treatment by YQJPF Decoction (**Fig. 5A, Table S17**).

### 3.3.5 Construction of PPI and Compound-Target-Disease network for potential therapeutic targets

The 163 potential therapeutic targets were uploaded to the STRING database, which provided the information on predicted interaction. Furthermore, we imported the above data into Cytoscape 3.7.1 to calculate the characteristics of the network and construct the protein-protein interaction network (PPI network) (**Fig. 5B**). In the PPI network, targets with higher degree played an important role in the protein-protein correlation. In **Fig. 5C**, ranked by degree value, 18 targets were collected to be the hub targets, namely VEGFA, EGFR, STAT3, CXCL8, ESR1, CCND1, PTPRC, MMP2, PECAM1, AR, SPP1, EDN1, CRP, F2, TIMP1, IRS1, HGF, CAV1, more details shown in **Table S18**. Then we built a Compound-Target-Disease network of complex information based on interactions between the drug (YQJPF), active compounds, and disease (ACLF) using Cytoscape to undertake visual analysis (**Fig. 5D**). In this network quercetin, resveratrol, syringaresinol diglucoside, luteolin, etc had higher degree value than other active compounds, connected to more than seven genes, so they would be the main active compounds to treat liver failure, more details shown in **Table 1**.

### 3.3.6 Analyses of Enrichment of the KEGG/GO Pathways

Gene ontology (GO), KEGG pathway enrichment analysis were performed in Metascape (<http://metascape.org>), with P Value  $< 0.01$ ; Enrichment  $> 1.5$ . GO enrichment analysis of the 163 potential therapeutic targets was performed for identifying the relevant biological functions of YQJPF against liver failure. The top 10 significantly enriched terms with a greater number of involved targets in biological process (BP), molecular function (MF) and cellular component (CC) categories were shown in **Fig. 5E**, which indicated that YQJPF may regulate oxidoreductase, nuclear receptor, get involved in wound healing, regeneration, metabolic process and so on. To explore the potential pathways of YQJPF on liver failure, the pathway enrichment of the 163 potential therapeutic targets was performed. The top 20 significantly enriched pathways were shown in **Fig. 5F**. Excluded pathways not related to liver disease or cancer-related pathways. PI3K/AKT, p53, FoxO, HIF-1, AMPK signaling pathways were the prominently enriched signaling pathways according to the gene count and P value (**Table S20**), which associated with inflammation, hypoxia, metabolism and proliferation. VEGF-A showed the highest degree value in hub targets. According to KEGG pathway enrichment analysis (**Table 2, Table S20**), apoptosis related genes BAX, Bcl-2 were closely related to the above pathways.

## 3.4 Effects of YQJPF on the hypoxic and apoptosis pathways

According to the network pharmacology analysis results, PI3K-AKT, HIF-1 $\alpha$  were the primary pathways, VEGF-A was identified as the primary drug candidate targets for the treatment of YQJPF on liver failure, and it was a downstream target marker of HIF-1 $\alpha$ , hypoxia-related cell injury plays an important role in acute and chronic liver failure[[\[ii\]](#)]. HIF-1 and VEGF-A increase under hypoxic conditions, act as a mediator for cell adaptation to a harmful environment. So we further investigated the mechanism of YQJPF on relieving liver injury by examining the protein levels in CCl<sub>4</sub> and LPS/D-gal induced ACLF model rats. YQJPF upregulated the expression of PI3K, AKT, HIF-1 $\alpha$ , VEGF-A. Besides, YQJPF increased HIF-1 $\alpha$  and VEGF-A expression by immunohistochemistry analysis, which indicated that hypoxic pathway significantly enhanced after YQJPF treatment. Moreover The expression of BCL-2, and BAX followed the same trend as the in vitro study results. Taken together, these findings may indicate that the mechanism of YQJPF on ACLF may through PI3K/AKT signaling pathway, modulate the the expression of HIF-1 $\alpha$ , VEGF-A, and apoptosis associated BCL-2, BAX. YQJPF could ameliorates liver injury through influencing hypoxia damage and apoptosis (**Fig. 6A**).

## 4. Discussion

Acute-on-chronic liver failure (ACLF) is a major worldwide medical problem, the worldwide reported mortality of ACLF according to the European Association for the Study of the Liver-Chronic Liver Failure (EASL-CLIF) Consortium definition ranges between 30% to 50%. Medical management of ACLF consists of early recognition, treatment of the precipitating event and supportive care, which includes antibacterial therapy, HBV-specific therapy, immunomodulation, extracorporeal liver support systems and liver transplantation<sup>[1]</sup>. However, there is still no significant increase in the availability of new drugs for improving liver injury, and alternative therapies are required to develop approaches to treat ACLF, such as TCM.

YQJPF is a traditional medicine formula, which proven to have a good therapeutic effect in clinical practice. In vivo experiments had confirmed that YQJPF can alleviate liver necrosis and fibrosis. Meanwhile YQJPF could promote proliferation and inhibit apoptosis in vitro. In order to get a better understanding of mechanism, a series of control experiments were conducted. In network pharmacology, there were 135 active components among the 9 herbs in YQJPF, including quercetin, resveratrol, kaempferol, luteolin, which considered to be the major components(**Fig. 3B**), and denmonstrated to have effect on various liver diseases. Quercetin had been reported could alleviate ethanol-induced liver steatosis[[\[i\]](#)], and hepatocytes damage[[\[ii\]](#)], aslo had a chemopreventive effect on the liver-induced preneoplastic lesions in rats[[\[iii\]](#)]. Resveratrol was confirmed the protective effects on liver injury in a rat model of partial hepatectomy[[\[iv\]](#)], it could improve CCL<sub>4</sub>-induced liver fibrosis[[\[v\]](#)], and ameliorates lipid droplet accumulation in liver to cure non-alcoholic fatty liver disease (NAFLD)[[\[vi\]](#)]. Kaempferol could protect mice from D-Gal/LPS-induced acute liver failure [[\[vii\]](#)], liver fibrosis[[\[viii\]](#)], acute alcoholic liver injury[[\[ix\]](#)] and liver cancer[[\[x\]](#)]. Luteolin attenuated chronic liver injury induced by mercuric chloride[[\[xi\]](#)], protected against acute liver injury through regulation of inflammatory mediators and antioxidative enzymes[[\[xii\]](#)], promoted cell apoptosis by inducing autophagy in hepatocellular carcinoma[[\[xiii\]](#)].

Among the putative targets of YQJPF associate with liver failure, VEGF-A, EGFR, STAT3, CXCL8 were examples of relatively important targets evaluated by topological parameters, which were involved in PI3K/AKT, p53, FoxO, HIF-1, AMPK signaling pathways. PI3K/AKT pathway plays an essential role in cell metabolism, growth, apoptosis suppression and angiogenesis, PI3K/AKT [[\[xiv\]](#)],[[\[xv\]](#)],[[\[xvi\]](#)] pathway had been demonstrated to have effect on liver failure. Li et al[[\[xvii\]](#)], has discovered that hepatocytes pyroptosis could be inhibited through the PI3K/AKT pathway in liver I/R injury. The downstream effectors of PI3K/AKT include the pro-apoptotic protein Bax, and the anti-apoptotic protein Bcl2, activated AKT [[\[xviii\]](#)],[[\[xix\]](#)] can inhibit Bad, reduce apoptosis and exert hepatocyte protection[[\[xx\]](#)],[[\[xxi\]](#)]. We found that, similar to that reported about hepatocyte apoptosis, LPS combined with D-Gal was used to establish the rat model of ACLF, LPS to induce hepatocytes apoptosis[[\[xxii\]](#)] in this study. YQJPF increased the protein level of PI3K and further promoted the phosphorylation of Akt in liver tissues (**Fig. 6**). YQJPF administration activates Bcl2, reduces BAX, and shifts the BAX/Bcl2 ratio in a anti-apoptotic direction, in order to protect cells from apoptosis, similar results were also demonstrated in vitro studies. Previous studies have shown that HIF-1 $\alpha$  is subjected to regulation by the PI3K/Akt signaling pathway, especially under hypoxia condition, PI3K/HIF pathway plays a important role in cardio-protection and neuro-protection. This relationship has also been shown in the pathogenesis of several forms of liver disease, a number of mechanisms have been proposed for the protective effect of HIF-1. HIF-1 has been found to protect cells from hypoxic injury by promoting nutrient and O<sub>2</sub> transport via inducing the expression of downstream proteins such as VEGF[[\[xxiii\]](#)], which promote angiogenesis[[\[xxiv\]](#)]. After administration with YQJPF, the expressions of HIF-1 $\alpha$  and VEGF-A were increased, which were further confirmed by immunostaining and Western blot analysis. Therefore, the anti-liver failure effect of YQJPF may involve in the regulation of the HIF-1 $\alpha$ /VEGF-A and apoptosis signaling pathways. These results suggest that YQJPF is beneficial for alleviating liver failure, may regulate hypoxic liver injury through PI3K/AKT-HIF1 $\alpha$  dependent apoptosis pathway. More experiments are necessary to verify the mechanisms of YQJPF on hepatocyte injury.

## 5. Conclusion

In summary, we evaluated active compounds and possible targets in YQJPF to treat liver failure by network pharmacology and transcriptomics analysis. Moreover we establised a CCl<sub>4</sub> and LPS/D-gal induced ACLF rat model and LPS induced hepatocytes model to verify the effect and mechanism in vivo and in vitro. These results showed that YQJPF could treat liver failure in rats by regulating hepatocyte apoptosis and hypoxic injury through PI3K/AKT pathway. Our more in-depth work will focus on verifying compound's targets and pathways.

## Abbreviations

YQJPF, Yiqijianpi formula;

TCM, Traditional Chinese Medicine;

ACLF, Acute-on-chronic liver failure;

HPLC, High Performance Liquid Chromatography;

TCMSP, Traditional Chinese Medicine Systems Pharmacology Database and Analysis Platform;

TCMID, Traditional Chinese Medicine Integrated Database;

OB, Oral bioavailability;

DL, Drug-likeness;

CNKI, Chinese National Knowledge Infrastructure;

CCl<sub>4</sub>, Carbon tetrachloride;

DEGs, Differentially expressed genes;

KEGG, Kyoto Encyclopedia of Genes and Genomes;

GO, Gene Ontology;

ALT, Alanine aminotransferase;

AST, Aspartate aminotransferase;

H&E, Haematoxylin and eosin;

HIF-1 $\alpha$ , Hypoxia-inducible factor-1 $\alpha$ ;

VEGF, Vascular endothelial growth factor;

Bcl-2, B-cell lymphoma-2;

PI3K, Phosphatidylinositol 3-kinase

MP, Methylprednisolone

D-Gal, D-Galactosamine;

LPS, Lipopolysaccharide

## Declarations

### Acknowledgments

We thank all family members, friends and workmates for their help, wish them good health and happiness.

### Author contributions

TSZ, ZSZ and ZF contributed to conception and design of the study. TL wrote and contributed to the writing of the manuscript. TL, XLY, WFX performed histological detection, western blot and the kits analysis. XSW conducted animal experiments. SM and ZLL conducted the network pharmacology analysis. TL and TSZ revises and collates the manuscript. All authors read and approved the final manuscript.

### Funding

This work was supported by the Leading Talent Project of Jiangsu Province Traditional Chinese Medicine (SLJ0216) and Research Fund of the Nanjing Hospital of Chinese Medicine Affiliated to Nanjing University of Chinese Medicine (YJJC201909).

### Availability of data and materials

The datasets used in the current study are available from the corresponding author on reasonable request.

### Conflict of interest statement

We declare that we have no financial and personal relationships with other people or organizations that can inappropriately influence our work, there is no professional or other personal interest of any nature or kind in any product, service and/or company that could be construed as influencing the position presented in.

### Ethics approval and consent to participate

This study was implemented in accordance with the standards of animal care as outlined in the Guide for the Care and Use of Laboratory Animals introduced by the U.S. National Institutes of Health (NIH Publication No.85-23, revised 1996). The animal protocol used in this study was approved by the institutional and local committee on the care and use of animals of the Nanjing University of Traditional Chinese Medicine (Nanjing, China), permission number 201903A012.

### Consent for publication

All authors consent to the publication of this manuscript. Neither the article nor portions of it have been previously published elsewhere.

### Competing interests

All authors declare no conflicts of interest.

## References

1. Moreau, R. Jalan, P. Gines, M. et al. Arroyo, CANONIC Study Investigators of the EASL–CLIF Consortium, Acute-on-chronic liver failure is a distinct syndrome that develops in patients with acute decompensation of cirrhosis, *Gastroenterology*. 144 (2013) 1426–1437, 1437.e1–9. <https://doi.org/10.1053/j.gastro.2013.02.042>.
2. Arroyo, R. Moreau, R. Jalan, P. Gines, EASL-CLIF Consortium CANONIC Study, Acute-on-chronic liver failure: A new syndrome that will re-classify cirrhosis, *Journal of Hepatology*. 62 (2015) S131-143. <https://doi.org/10.1016/j.jhep.2014.11.045>.
3. K. Sarin, A. Choudhury, M.K. Sharma, R. Maiwall, M. Al Mahtab, S. Rahman, et al, APASL ACLF Research Consortium (AARC) for APASL ACLF working Party., Acute-on-chronic liver failure: consensus recommendations of the Asian Pacific association for the study of the liver (APASL): an update, *Hepatology International*. 13 (2019) 353–390. <https://doi.org/10.1007/s12072-019-09946-3>.
4. L. Hopkins, Network pharmacology: the next paradigm in drug discovery, *Nature Chemical Biology*. 4 (2008) 682–690. <https://doi.org/10.1038/nchembio.118>.
5. Moreau, R. Jalan, P. Gines, M. et al, CANONIC Study Investigators of the EASL–CLIF Consortium, Acute-on-chronic liver failure is a distinct syndrome that develops in patients with acute decompensation of cirrhosis, *Gastroenterology*. 144 (2013) 1426–1437, 1437.e1–9. <https://doi.org/10.1053/j.gastro.2013.02.042>.
6. Shi, Y. Yang, Y. Hu, W. et al, Acute-on-chronic liver failure precipitated by hepatic injury is distinct from that precipitated by extrahepatic insults, *Hepatology* (Baltimore, Md.). 62 (2015) 232–242. <https://doi.org/10.1002/hep.27795>.
7. Li, L.-Y. Chen, N.-N. Zhang, S.-T. Li, B. Zeng, M. Pavesi, À. Amorós, R.P. Mookerjee, Q. Xia, F. Xue, X. Ma, J. Hua, L. Sheng, D.-K. Qiu, Q. Xie, G.R. Foster, G. Dusheiko, R. Moreau, P. Gines, V. Arroyo, R. Jalan, Characteristics, Diagnosis and Prognosis of Acute-on-Chronic Liver Failure in Cirrhosis Associated to Hepatitis B, *Scientific Reports*. 6 (2016) 25487. <https://doi.org/10.1038/srep25487>.
8. Shahzad M, Shabbir A, Wojcikowski K, Wohlmuth H, Gobe GC. The Antioxidant Effects of Radix Astragali (*Astragalus membranaceus* and Related Species) in Protecting Tissues from Injury and Disease. *Curr Drug Targets*. 2016;17(12):1331-40. doi: 10.2174/1389450116666150907104742. PMID: 26343107.
9. Shan H, Zheng X, Li M. The effects of *Astragalus Membranaceus* Active Extracts on Autophagy-related Diseases. *Int J Mol Sci*. 2019 Apr 17;20(8):1904. doi: 10.3390/ijms20081904. PMID: 30999666; PMCID: PMC6514605.
10. Chen Z, Li S, Wang X, Zhang CL. Protective effects of Radix *Pseudostellariae* polysaccharides against exercise-induced oxidative stress in male rats. *Exp Ther Med*. 2013 Apr;5(4):1089-1092. doi: 10.3892/etm.2013.942. Epub 2013 Jan 31. PMID: 23596474; PMCID: PMC3628077.
11. Fang Z, Hu X, Chen Z, Xie J, Wu D, Yin Y, You L. Radix *pseudostellariae* of Danzhi Jiangtang capsule relieves oxidative stress of vascular endothelium in diabetic macroangiopathy. *Saudi Pharm J*. 2020 Jun;28(6):683-691. doi: 10.1016/j.jsps.2020.04.009. Epub 2020 May 6. PMID: 32550799; PMCID: PMC7292866.
12. Liu Z, Sun Y, Zhang J, Ou N, Gu P, Hu Y, Liu J, Wu Y, Wang D. Immunopotential of Polysaccharides of *Atractylodes macrocephala* Koidz-loaded nanostructured lipid carriers as an adjuvant. *Int J Biol Macromol*. 2018 Dec;120(Pt A):768-774. doi: 10.1016/j.ijbiomac.2018.08.108. Epub 2018 Aug 23. PMID: 30144550.
13. Cao P, Sun J, Sullivan MA, Huang X, Wang H, Zhang Y, Wang N, Wang K. *Angelica sinensis* polysaccharide protects against acetaminophen-induced acute liver injury and cell death by suppressing oxidative stress and hepatic apoptosis in vivo and in vitro. *Int J Biol Macromol*. 2018 May;111:1133-1139. doi: 10.1016/j.ijbiomac.2018.01.139. Epub 2018 Feb 19. Erratum in: *Int J Biol Macromol*. 2018 May 10; PMID: 29415408.
14. Chen Q, Liu M, Yu H, Li J, Wang S, Zhang Y, Qiu F, Wang T. *Scutellaria baicalensis* regulates FFA metabolism to ameliorate NAFLD through the AMPK-mediated SREBP signaling pathway. *J Nat Med*. 2018 Jun;72(3):655-666. doi: 10.1007/s11418-018-1199-5. Epub 2018 Mar 14. PMID: 29542003.
15. Seo HL, Baek SY, Lee EH, Lee JH, Lee SG, Kim KY, Jang MH, Park MH, Kim JH, Kim KJ, Lee HS, Ahn SC, Lee JR, Park SJ, Kim SC, Kim YW. *Liquistri lucidi* Fructus inhibits hepatic injury and functions as an antioxidant by activation of AMP-activated protein kinase in vivo and in vitro. *Chem Biol Interact*. 2017 Jan 25;262:57-68. doi: 10.1016/j.cbi.2016.11.031. Epub 2016 Dec 1. PMID: 27916511.
16. Yang Zhang, Yinya Wu, Shanzhong Tan, Xiao Qian, Jianjun Shen, Chongfeng Liang, Shulian Jiang, Clinical Observation on Chronic Severe Hepatitis B Treated by Principle of Strengthening Vital Qi and the Spleen Based on the Mechanism of Deficiency in Vital Qi, *Zhong Guo Zhong Yi Ji Zheng*. 21 (2012) 872-873+892.
17. L. Hopkins, Network pharmacology: the next paradigm in drug discovery, *Nature Chemical Biology*. 4 (2008) 682–690. <https://doi.org/10.1038/nchembio.118>.



18. Ni, S. Li, N. Yang, X. Tang, S. Zhang, D. Hu, M. Lu, Deregulation of Regulatory T Cells in Acute-on-Chronic Liver Failure: A Rat Model, *Mediators Inflamm.* 2017 (2017). <https://doi.org/10.1155/2017/1390458>.
19. Heil, D. Schultze, P. Schemmer, H. Bruns, N-acetylcysteine protects hepatocytes from hypoxia-related cell injury, *Clinical and Experimental Hepatology.* 4 (2018) 260–266. <https://doi.org/10.5114/ceh.2018.80128>.
20. Zeng, X. Guo, F. Zhou, L. Xiao, J. Liu, C. Jiang, M. Xing, P. Yao, Quercetin alleviates ethanol-induced liver steatosis associated with improvement of lipophagy, *Food and Chemical Toxicology: An International Journal Published for the British Industrial Biological Research Association.* 125 (2019) 21–28. <https://doi.org/10.1016/j.fct.2018.12.028>.
21. Lee, J. Lee, H. Lee, J. Sung, Relative protective activities of quercetin, quercetin-3-glucoside, and rutin in alcohol-induced liver injury, *Journal of Food Biochemistry.* 43 (2019) e13002. <https://doi.org/10.1111/jfbc.13002>.
22. Carrasco-Torres, H.C. Monroy-Ramírez, A.A. Martínez-Guerra, R. Baltiérrez-Hoyos, M. de L.Á. Romero-Tlalolini, S. Villa-Treviño, X. Sánchez-Chino, V.R. Vásquez-Garzón, Quercetin Reverses Rat Liver Preneoplastic Lesions Induced by Chemical Carcinogenesis, *Oxidative Medicine and Cellular Longevity.* 2017 (2017) 4674918. <https://doi.org/10.1155/2017/4674918>.
23. Yu, X. Zhou, H. Xiang, S. Wang, Z. Cui, J. Zhou, Resveratrol Reduced Liver Damage After Liver Resection in a Rat Model by Upregulating Sirtuin 1 (SIRT1) and Inhibiting the Acetylation of High Mobility Group Box 1 (HMGB1), *Medical Science Monitor: International Medical Journal of Experimental and Clinical Research.* 25 (2019) 3212–3220. <https://doi.org/10.12659/MSM.913937>.
24. Yu, S.-Y. Qin, B.-L. Hu, Q.-Y. Qin, H.-X. Jiang, W. Luo, Resveratrol improves CCL4-induced liver fibrosis in mouse by upregulating endogenous IL-10 to reprogramme macrophages phenotype from M(LPS) to M(IL-4), *Biomedicine & Pharmacotherapy = Biomedecine & Pharmacotherapie.* 117 (2019) 109110. <https://doi.org/10.1016/j.biopha.2019.109110>.
25. Zhou, L. Yi, X. Ye, X. Zeng, K. Liu, Y. Qin, Q. Zhang, M. Mi, Resveratrol Ameliorates Lipid Droplet Accumulation in Liver Through a SIRT1/ATF6-Dependent Mechanism, *Cellular Physiology and Biochemistry: International Journal of Experimental Cellular Physiology, Biochemistry, and Pharmacology.* 51 (2018) 2397–2420. <https://doi.org/10.1159/000495898>.
26. Wang, L. Chen, X. Zhang, L. Xu, B. Xie, H. Shi, Z. Duan, H. Zhang, F. Ren, Kaempferol protects mice from d-GalN/LPS-induced acute liver failure by regulating the ER stress-Grp78-CHOP signaling pathway, *Biomedicine & Pharmacotherapy = Biomedecine & Pharmacotherapie.* 111 (2019) 468–475. <https://doi.org/10.1016/j.biopha.2018.12.105>.
27. Xu, S. Huang, Q. Huang, Z. Ming, M. Wang, R. Li, Y. Zhao, Kaempferol attenuates liver fibrosis by inhibiting activin receptor-like kinase 5, *Journal of Cellular and Molecular Medicine.* 23 (2019) 6403–6410. <https://doi.org/10.1111/jcmm.14528>.
28. Chen, Y.-H. Xuan, M.-X. Luo, X.-G. Ni, L.-Q. Ling, S.-J. Hu, J.-Q. Chen, J.-Y. Xu, L.-Y. Jiang, W.-Z. Si, L. Xu, H. Gao, Z. Liu, H. Li, Kaempferol alleviates acute alcoholic liver injury in mice by regulating intestinal tight junction proteins and butyrate receptors and transporters, *Toxicology.* 429 (2020) 152338. <https://doi.org/10.1016/j.tox.2019.152338>.
29. Zhu, X. Liu, H. Li, Y. Yan, X. Hong, Z. Lin, Kaempferol inhibits proliferation, migration, and invasion of liver cancer HepG2 cells by down-regulation of microRNA-21, *International Journal of Immunopathology and Pharmacology.* 32 (2018) 2058738418814341. <https://doi.org/10.1177/2058738418814341>.
30. Zhang, X. Tan, D. Yang, J. Lu, B. Liu, R. Baiyun, Z. Zhang, Dietary luteolin attenuates chronic liver injury induced by mercuric chloride via the Nrf2/NF-κB/P53 signaling pathway in rats, *Oncotarget.* 8 (2017) 40982–40993. <https://doi.org/10.18632/oncotarget.17334>.
31. [[1]]M. Park, Y.-S. Song, Luteolin and luteolin-7-O-glucoside protect against acute liver injury through regulation of inflammatory mediators and antioxidative enzymes in GalN/LPS-induced hepatitic ICR mice, *Nutrition Research and Practice.* 13 (2019) 473–479. <https://doi.org/10.4162/nrp.2019.13.6.473>.
32. Cao, H. Zhang, X. Cai, W. Fang, D. Chai, Y. Wen, H. Chen, F. Chu, Y. Zhang, Luteolin Promotes Cell Apoptosis by Inducing Autophagy in Hepatocellular Carcinoma, *Cellular Physiology and Biochemistry: International Journal of Experimental Cellular Physiology, Biochemistry, and Pharmacology.* 43 (2017) 1803–1812. <https://doi.org/10.1159/000484066>.
33. Li, L. Lu, N. Luo, Y.-Q. Wang, H.-M. Gao, Inhibition of PI3K/Akt/mTOR signaling pathway protects against d-galactosamine/lipopolysaccharide-induced acute liver failure by chaperone-mediated autophagy in rats, *Biomedicine & Pharmacotherapy = Biomedecine & Pharmacotherapie.* 92 (2017) 544–553. <https://doi.org/10.1016/j.biopha.2017.05.037>.
34. Zhong, K. Qian, J. Xiong, K. Ma, A. Wang, Y. Zou, Curcumin alleviates lipopolysaccharide induced sepsis and liver failure by suppression of oxidative stress-related inflammation via PI3K/AKT and NF-κB related signaling, *Biomedicine & Pharmacotherapy = Biomedecine & Pharmacotherapie.* 83 (2016) 302–313. <https://doi.org/10.1016/j.biopha.2016.06.036>.
35. Caracul, E. Sastre, P. Llénenes, I. Prieto, T. Funes, M.Á. Aller, J. Arias, G. Balfagón, J. Blanco-Rivero, Acute-on-chronic liver disease enhances phenylephrine-induced endothelial nitric oxide release in rat mesenteric resistance arteries through enhanced PKA, PI3K/AKT and cGMP signalling pathways, *Scientific Reports.* 9 (2019) 6993. <https://doi.org/10.1038/s41598-019-43513-y>.
36. Li, F. Zhao, Y. Cao, J. Zhang, P. Shi, X. Sun, F. Zhang, L. Tong, DHA attenuates hepatic ischemia reperfusion injury by inhibiting pyroptosis and activating PI3K/Akt pathway, *Eur J Pharmacol.* 835 (2018) 1–10. <https://doi.org/10.1016/j.ejphar.2018.07.054>.
37. Wang, J. Pan, D. Liu, M. Zhang, X. Li, J. Tian, M. Liu, T. Jin, F. An, Nicorandil alleviates apoptosis in diabetic cardiomyopathy through PI3K/Akt pathway, *J Cell Mol Med.* 23 (2019) 5349–5359. <https://doi.org/10.1111/jcmm.14413>.
38. Shariati, F. Meric-Bernstam, Targeting AKT for cancer therapy, *Expert Opin Investig Drugs.* 28 (2019) 977–988. <https://doi.org/10.1080/13543784.2019.1676726>.
39. Jin, H. Gao, J. Wang, S. Yang, J. Wang, J. Liu, Y. Yang, T. Yan, T. Chen, Y. Zhao, Y. He, Role and regulation of autophagy and apoptosis by nitric oxide in hepatic stellate cells during acute liver failure, *Liver International: Official Journal of the International Association for the Study of the Liver.* 37 (2017)

1651–1659. <https://doi.org/10.1111/liv.13476>.

40. -Z. Li, Z.-Y. Liao, Y.-X. Li, Z.-Y. Ming, J.-H. Zhong, G.-B. Wu, S. Huang, Y.-N. Zhao, A20 rescues hepatocytes from apoptosis through the NF-κB signaling pathway in rats with acute liver failure, *Bioscience Reports*. 39 (2019). <https://doi.org/10.1042/BSR20180316>.

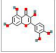
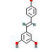
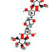
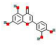
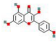
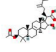
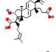
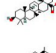

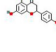
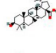
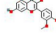
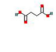
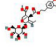
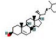
41. Chen, Z. Wu, B. Yuan, Y. Dong, L. Zhang, Z. Zeng, MicroRNA-146a-5p attenuates irradiation-induced and LPS-induced hepatic stellate cell activation and hepatocyte apoptosis through inhibition of TLR4 pathway, *Cell Death & Disease*. 9 (2018) 22. <https://doi.org/10.1038/s41419-017-0038-z>.

42. Bocca, E. Novo, A. Miglietta, M. Parola, Angiogenesis and Fibrogenesis in Chronic Liver Diseases, *Cellular and Molecular Gastroenterology and Hepatology*. 1 (2015) 477–488. <https://doi.org/10.1016/j.jcmgh.2015.06.011>.

43. Nath, G. Szabo, Hypoxia and hypoxia inducible factors: diverse roles in liver diseases, *Hepatology*. 55 (2012) 622–633. <https://doi.org/10.1002/hep.25497>.

## Tables

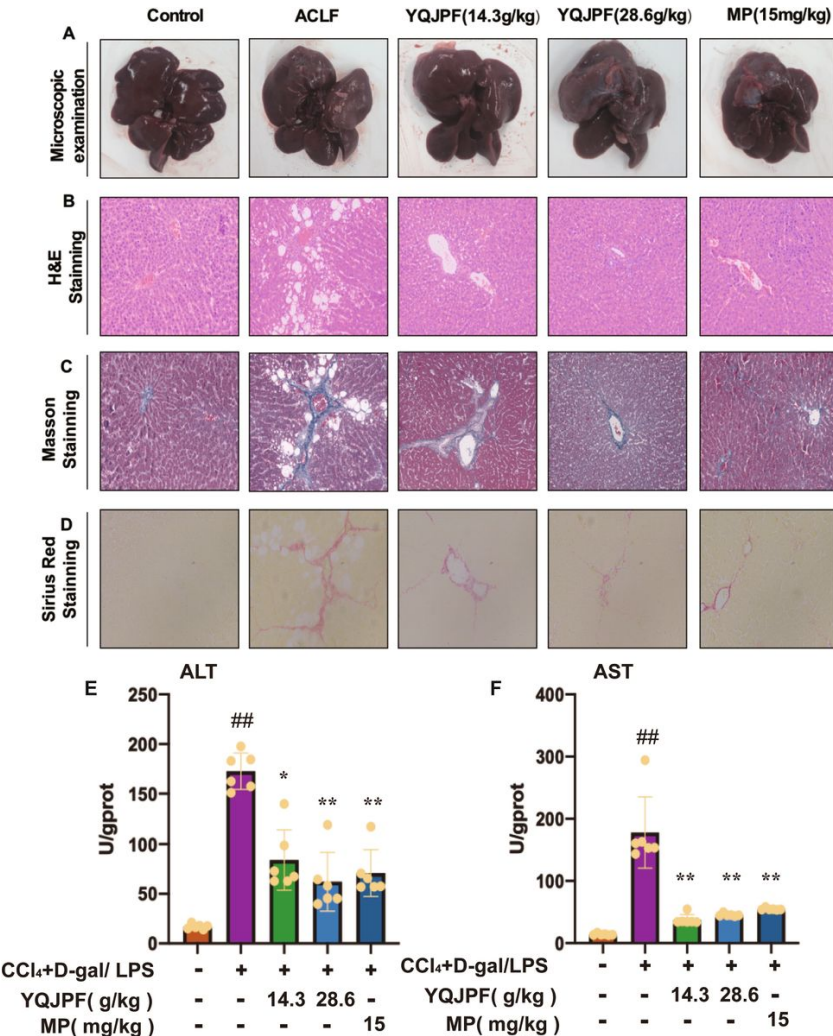
**Table1: The top 15 bioactive compounds of YQJPF are listed below according to the degree of similarity of the compound–disease–target networks**

Compound Name	Pubchem ID	Herbal	OB%	DL	Structure
Quercetin	5280343	Astragalus membranaceus	46.43	0.28	
Resveratrol	445154	Astragalus membranaceus	19.07	0.11	
Syringaresinol Diglucoside	442830	Fructus Ligustri Lucidi	83.12	0.8	
Luteolin	5280445	Radix pseudostellariae, Fructus Ligustri Lucidi	36.16	0.23	
Kaempferol	5280863	Astragalus membranaceus, Fructus Ligustri Lucidi	41.88	0.24	
Pachymic acid	5484385	Poria Wolfiporia extensa	33.63	0.81	
Pericosic acid B	5471852	Poria Wolfiporia extensa	30.52	0.75	
Ursolic acid	64945	Radix pseudostellariae	16.46	0.75	
Pericosic acid A	5471851	Poria Wolfiporia extensa	30.61	0.76	
Naringenin	932	Pericarpium citri reticulatae	59.29	0.21	
Maizin	64971	Astragalus membranaceus	55.38	0.78	
Isohammetin	5281654	Astragalus membranaceus	49.6	0.31	
Succinic acid	1110	Radix pseudostellariae	29.63	0.01	
Lucidanoside D	10531060	Fructus Ligustri Lucidi	48.87	0.71	
Beta-sitosterol	222284	Radix pseudostellariae, Angelica sinensis, Fructus Ligustri Lucidi, Scutellaria baicalensis	36.91	0.75	

**Table 2: Prominently enriched signaling pathways**

Term	Ratio	pvalue	Count	Gene
PI3K-Akt signaling pathway	5.263157895	1.76226E-11	18	CCND1,BCL2,CCND2,CCNE1,CHUK,COL1A1,EGFR,FGF1,HGF,INSR,IRS1,JAK1,MDM2,MET,PIK3CG,RXRA,S
HIF-1 signaling pathway	9.900990099	1.54787E-09	10	BCL2,EDN1,EGFR,HMOX1,INSR,PFKFB3,PRKCB,STAT3,TIMP1,VEGFA
Apoptosis	7.246376812	3.22327E-08	10	BIRC5,BAX,BCL2,BCL2A1,CHUK,CTSB,CTSD,CTSK,PMAIP1,CFLAR

Figures



**Figure 1**

YQJPF protected rats liver from CCl4-induced injury and ameliorated hepatic injury (A) Representative photograph of liver tissues; (B) H&E-stained sections of liver tissues (Scale bars, 100 μm) (C) Masson-stained sections of liver tissues. (Scale bars, 100 μm); (B) Sirius-Red stained sections of liver tissues. (Scale bars, 100 μm); (E-F) ELISA analysis of tissue ALT, AST levels. Data were expressed as mean ± SD (n = 6); \*P < 0.05 versus Model, \*\*P < 0.01 versus Model, ##P < 0.01 versus vehicle control. The p-values were obtained using ANOVA.

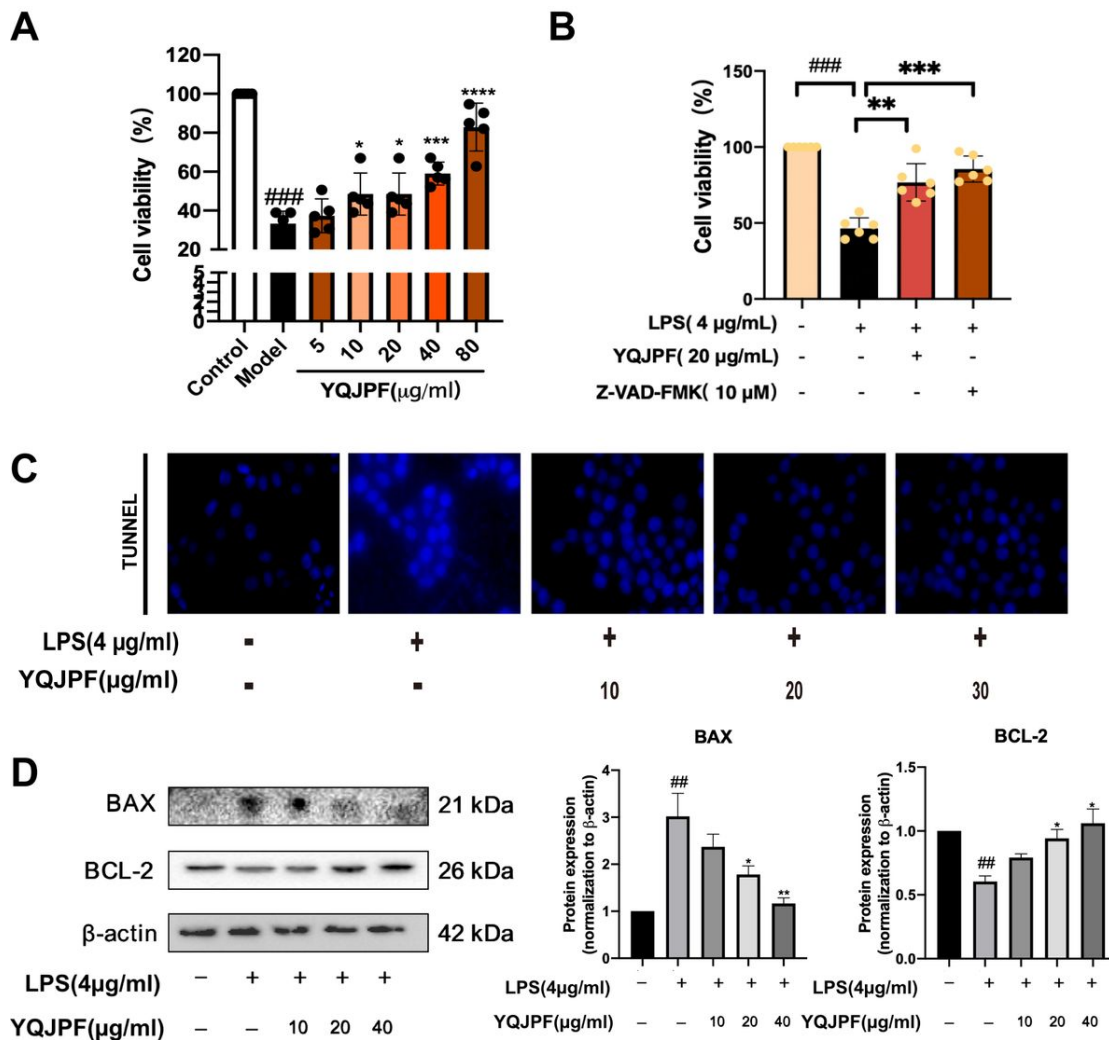
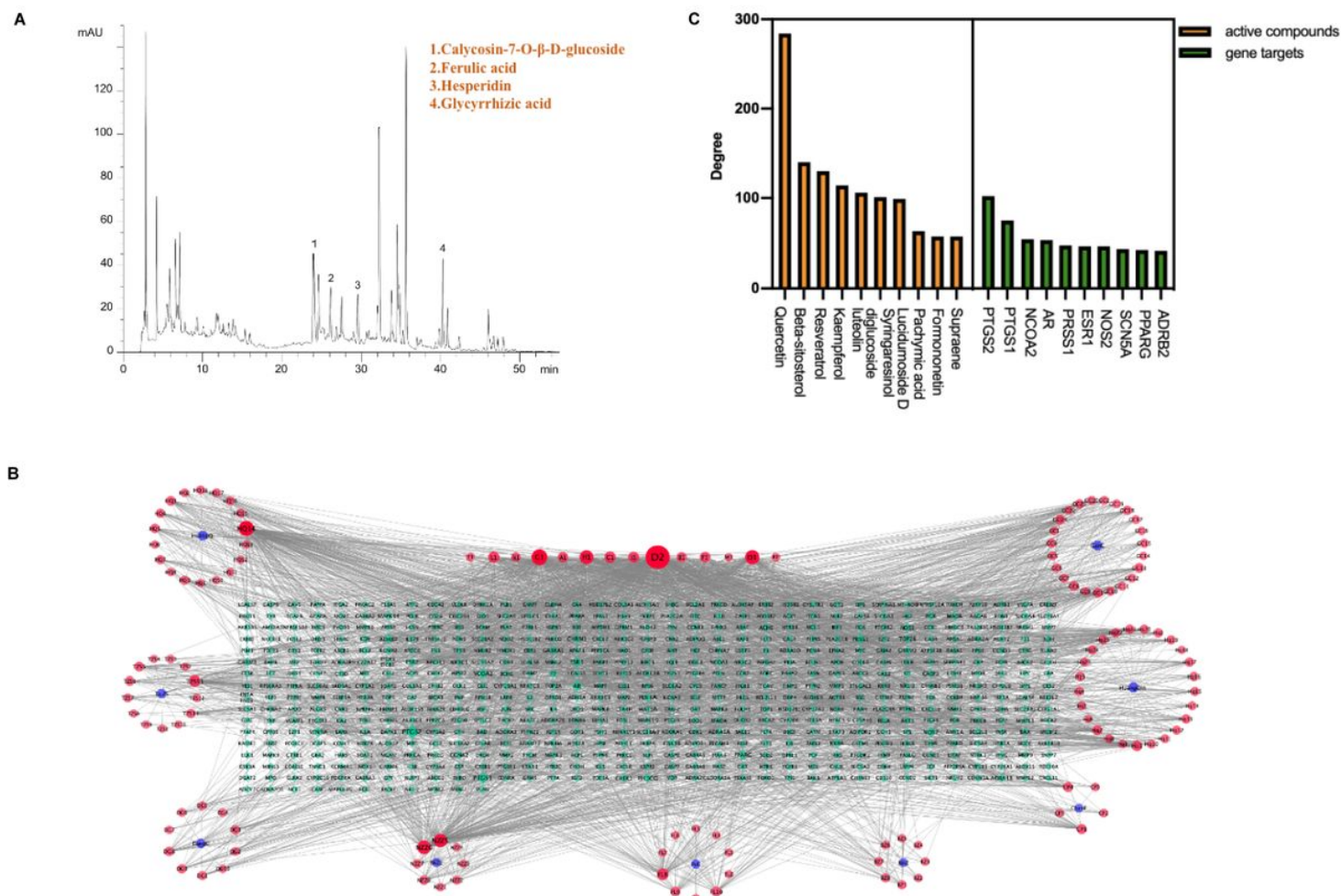


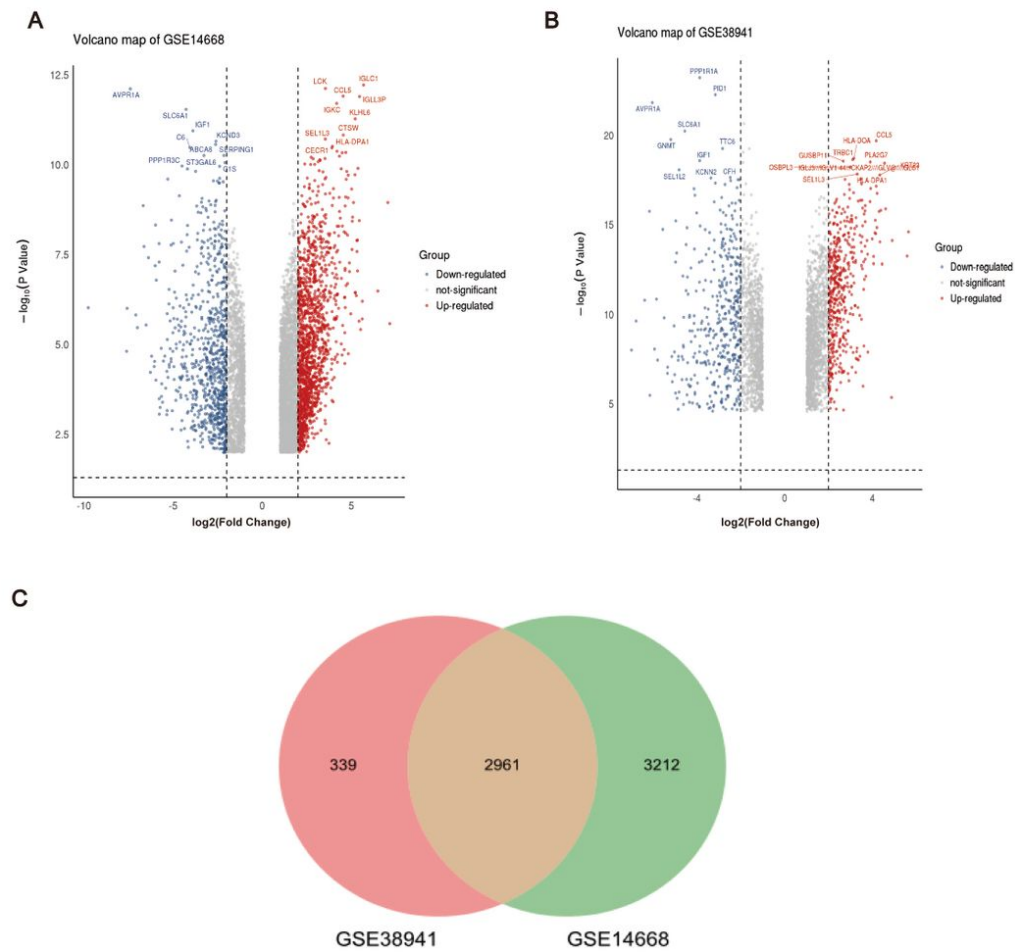
Figure 2

YQJPF promoted cell proliferation and inhibited apoptosis in vitro. Human L02 cells were treated with LPS (4µg/ml) or YQJPF at indicated concentrations for 24 h. (A) YQJPF significantly promoted cell proliferation in dose dependent manner as shown by Cell Counting Kit-8 analysis of the cell viability. (B-D) YQJPF can inhibit cell apoptosis, L02 cells were pretreated with 10 µM pan-caspase inhibitor Z-VAD-FMK, CCK-8 analysis was detected for cell viability. TUNEL staining was used to detect cell apoptosis. Scale bar, 100 µm. The expression of BAX decreased and Bcl-2 increased with YQJPF treatment, values were shown as the mean ± SD, \*p < 0.05, \*\*p < 0.01 vs. Model group. ##P < 0.01, ###P < 0.001 versus vehicle control. The p-values were obtained using ANOVA.



**Figure 3**

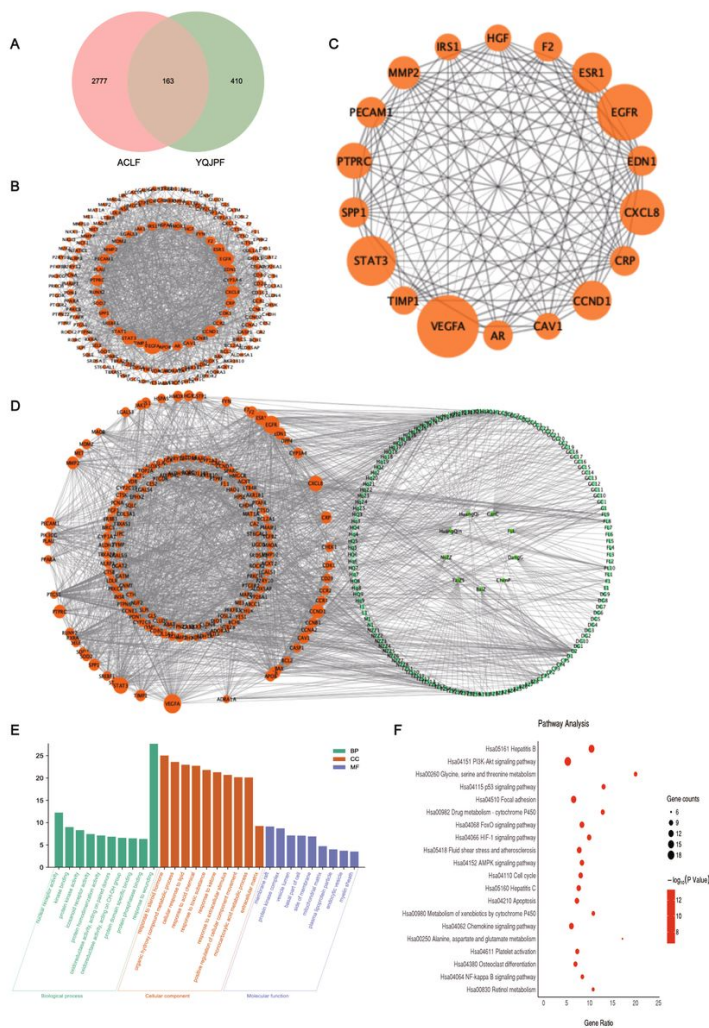
Active components and potential gene targets in YQJPF. (A) HPLC of YQJPF, four main compounds (Calycosin-7-O-β-D-glucoside, Ferulic acid, Hesperidin, Glycyrrhizic acid) were determined by Agilent 1260 liquid chromatography system. (B) The Compound-Target network of YQJPF. The orange nodes represented active compounds and the green nodes represented targets. Nodes size and color depth were proportional to their degree. The dots in a straight line represented the common components of more than two herbs. (C) Gene targets and active compounds with the top 10 degree values.



**Figure 4**

Therapeutic Gene Targets for Liver Failure:(A) Volcano map of differentially expressed genes for GSE14668. (B) Volcano map of differentially expressed genes for GSE38941. Red nodes represented up-regulated genes, while blue nodes represented down-regulated genes.(C) Venn diagram showed the overlapping genes between the two data sets (middle), which represented the therapeutic gene targets for Liver Failure.





**Figure 5**

Network pharmacological analysis and biological functional enrichment analysis of YQJPF. (A) Venn diagram showed 163 potential therapeutic targets of YQJPF in liver failure. (B) Protein-protein interaction (PPI) network of active compounds of YQJPF against liver failure. Nodes size were proportional to their degree. (C) Hub targets ranked by degree value in PPI network. Nodes size were proportional to their degree. (D) The compound-target network of YQJPF in liver failure. The green nodes represented active compounds and the orange nodes represented potential gene targets. The edges represented the interactions between them and nodes size were proposed. (E-F) Enrichment of the KEGG/GO Pathways.

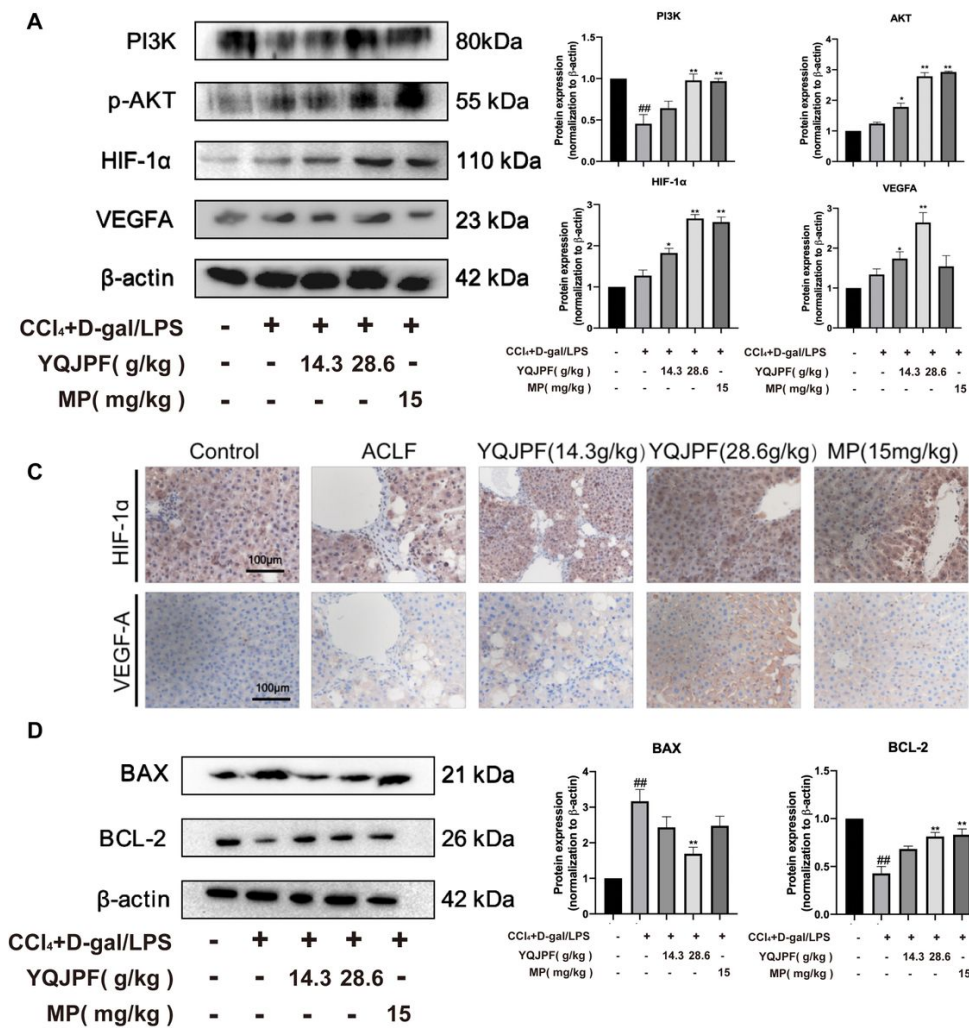
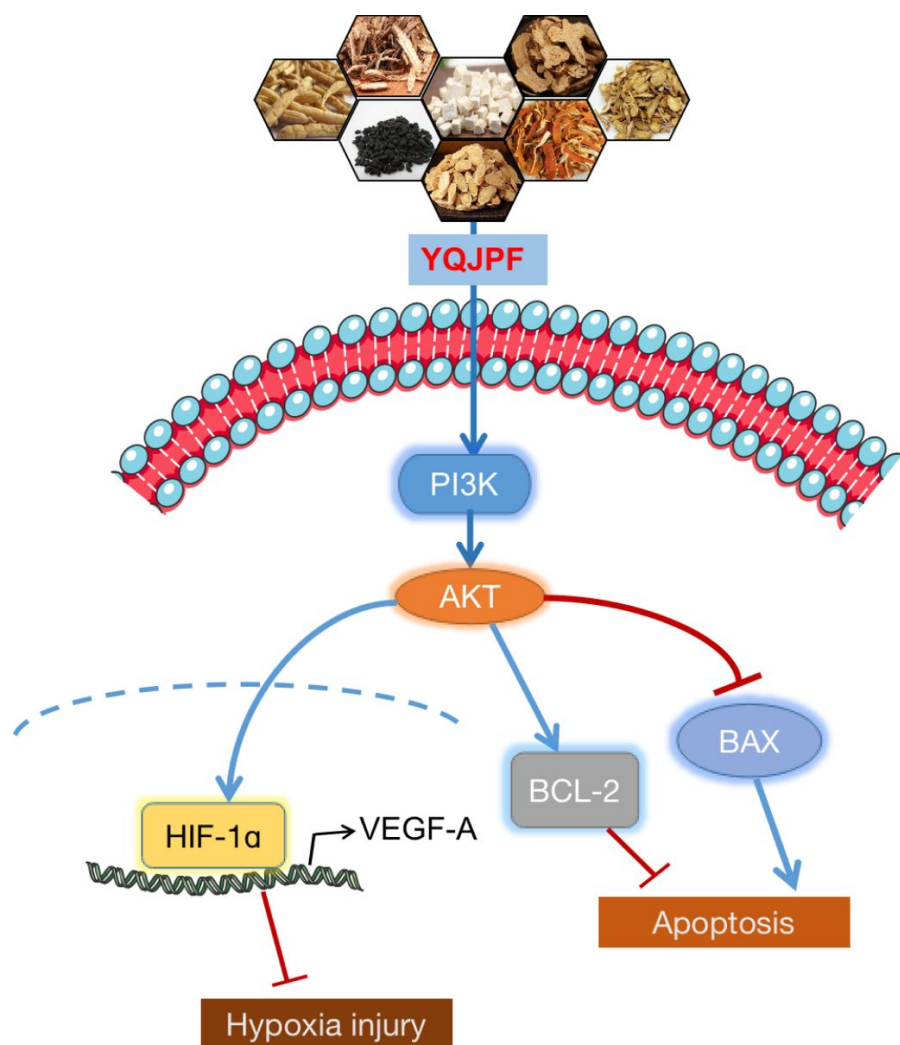


Figure 6

YQJPF modulated the expression of the PI3K/AKT/HIF-1 $\alpha$  and apoptosis signaling pathway proteins. (A-B) Protein expression levels of p-PI3K, p-AKT, HIF-1 $\alpha$  and VEGF-A in liver tissues. (C) IHC analysis of HIF-1 $\alpha$  and VEGF-A expression in YQJPF-treated liver tissues ( $\times 400$  magnification). (D) Protein expression levels of Bcl-2 and BAX. Values are shown as the mean  $\pm$  SD, #P < 0.05, ##P < 0.01 (vs. control group), \*P < 0.05, and \*\*P < 0.01 (vs. ACLF model group).





**Figure 7**

Hepatoprotective effect of Yiqijianpi formula (YQJPF) on liver failure through modulation of hypoxic and apoptosis pathway. By combining the network pharmacological analysis and our results, we hypothesized that YQJPF activates the PI3K/AKT signaling pathway and modulates the expression of HIF-1 $\alpha$  and BCL-2 family proteins, thereby alleviate liver hypoxia injury and apoptosis.

## Supplementary Files

This is a list of supplementary files associated with this preprint. Click to download.

- [figureabstract.tif](#)
- [SupplementaryTablesS1S11.xlsx](#)
- [Supplementarymaterials2TableS1213.docx](#)
- [SupplementaryTablesS12S19.xlsx](#)
- [supplementatymaterial4Tables20.xlsx](#)